Analytical model for viscous damping and the spring force for perforated planar microstructures acting at both audible and ultrasonic frequencies

Dorel Homentcovschi[a] and Ronald N. Miles
Department of Mechanical Engineering, SUNY Binghamton, Binghamton, NY 13902-6000

(Received 27 September 2007; revised 10 April 2008; accepted 10 April 2008)

The paper presents a model for the squeezed film damping, the resistance of the holes, and the corresponding spring forces for a periodic perforated microstructure including the effects of compressibility, inertia, and rarefied gas. The viscous damping and spring forces are obtained by using the continuity equation. The analytical formula for the squeezed film damping is applied to analyze the response of an ultrasonic transducer. The inclusion of these effects in a model significantly improves the agreement with measured results. Finally, it is shown that the frequency dependence of the total damping and total spring force for a cell are very similar to those corresponding to a rectangular open microstructure without holes. A separate analysis reveals the importance of each particular correction. The most important is the compressibility correction; the inertia has to be considered only for determining the spring force and the damping force for sufficiently high frequencies. © *2008 Acoustical Society of America.* [DOI: 10.1121/1.2918542]

PACS number(s): 43.38.Bs, 43.35.Ae [AJZ] Pages: 175–181

I. INTRODUCTION

Recent progress in micromachining technology has enabled the fabrication of microelectro-mechanical systems (MEMS), such as microphones, microaccelerometers, pressure sensors, switches, mirrors, tunable interferometers, ultrasonic motors, resonators, etc. MEMS devices often use parallel plate electrodes as the capacitive sensing and electrostatic actuation mechanisms. In order to increase sensitivity for sensing and to increase force for actuation, designers try to increase the electrode area and decrease the gap between plates. This type of device typically requires etch holes to reduce the time required to release the micromechanical structure during the etching of sacrificial materials. Therefore, the study of a thin air layer being squeezed between a moving plate and a perforated backplate, referred to as a perforated planar microstructure, is important in many MEMS.

As the movable electrode displaces sinusoidally, the sinusoidal backforce on the plate due to the air separating it from the backplate has two components:[1] The viscous damping force, which is in phase with velocity, and the spring force, which is in phase with the plate displacement.

Viscous damping is a critical factor for many MEMS transducers and actuators. In many applications sensors require low damping in order to achieve sufficient sensitivity of the system under a given driving force. In the case of microphones, the mechanical-thermal noise is often one of the limiting noise components. The magnitude of thermal noise depends only on temperature and the magnitude of mechanical damping.[2] Consequently, high viscous damping is also associated with large mechanical-thermal noise. Many devices need to be damped for stable operation. Therefore, in designing a MEMS device, the effects of viscous damping must be taken into account at the earliest stage.[3] The efficient etching, the proper value of the viscous damping, the control of the structure stiffness, and the electrical sensitivity are all directly influenced by the holes on the backplate. Consequently, MEMS design requires a comprehensive understanding of the micromachined perforated systems and their dynamic behavior.

While viscous forces dominate the mechanical behavior of planar microstructures at small velocities, the compressibility of the gas and inertial forces become important factors in determining the spring force at higher frequencies. The dynamic stiffness, the damping coefficients, and the transitional frequencies in compressible viscous thin films have been analyzed previously for the case of infinite strips, thin annuli, and circular plates. A detailed review was given by Andrews, Harris, and Turner.[4] In the case of perforated planar microstructures a similar analysis can be performed for mechanical structures containing a periodic system of holes. While the periodic hypothesis proves valid only in the case of infinite plates, the edge correction introduced in Ref. 5 permits one to assume periodicity (with a certain precision) for the inner cells of a finite domain containing a square web of aligned holes. Therefore, the theory developed in this paper can be applied to analyze real structures of a general shape.

In Sec. II the squeezed film damping is analyzed by taking into consideration the inertia, compressibility, and rarefaction effects. In the case where the basic domain is approximated by an annulus, the solution is obtained analytically. In Sec. III B the formulas obtained are applied to the analysis of the ultrasonic transducer developed by Oppen-

[a]Author to whom correspondence should be addressed. Permanent address: University Politechnica of Bucharest, Applied Science Department and Institute of Mathematical Statistics and Applied Mathematics of Romanian Academy, Calea 13 Septembrie #13, RO-76100, Bucharest, Romania. Electronic mail: homentco@binghamton.edu

heim, Jain, and Greve in Ref. 6. Consideration of compressibility, inertia, and rarefied gas effects reduced the error in predicting the quality factor of the damping of the diaphragm of the transducer from 48% to 14% as compared with the measured value.

In Sec. IV we first obtain a model for the direct resistance of a hole. The determination of the rim pressure p_1 is complicated by the compressibility of the gas and requires the consideration of the equation of continuity. Once the rim pressure is obtained, the total damping (and correspondingly the spring force) can be obtained by adding the squeezed film damping and the hole resistance under their complex form.[7] The example considered in Sec. IV C shows that the frequency dependence of the damping force and spring force for a cell are very similar to the corresponding elements determined by Veijola[8] for the case of rectangular plates without holes. Separate analysis of each special effect (compressibility, inertia, and rarefaction) shows that the most important is the compressibility factor. The inertia modifies the spring force and the damping coefficient only at high frequencies while the rarefaction correction has to be considered for gaps significantly thinner than 2 μm.

II. SQUEEZED FILM DAMPING

The complex three-dimensional (3D) motion of the air in a perforated planar microstructure can be decomposed in two simpler flows: a quasi-horizontal flow in the gap of the microstructure and a vertical (Poiseuille type) flow in the cylindrical holes. The presence of the holes implies two effects: a "*direct*" resistance of the holes obtained by adding the shear stress effect on the wall of the pipe (hole) and "*an indirect resistance of holes*" which changes the rim pressure (in the quasi-horizontal flow) from the value zero (corresponding to the external pressure) to a certain value "p_1" determined again by the resistance of the holes (see Ref. 5). The quasi-horizontal flow includes the squeeze film flow, corresponding to the zero pressure condition on the rim of the holes, and also the indirect hole resistance contribution due to the change of the pressure boundary condition to p_1. In this section both components are determined simultaneously.

A. Equations of the problem

In order to study the viscous damping in the gap of a planar microstructure we consider the continuity and the momentum equations for a viscous compressible gas.[7] The system has to be completed by a state equation. The relationship between the pressure and density at any point in the gas is assumed as described by a polytropic process with exponent n_γ

$$p\rho^{-n_\gamma} = const.$$

In the case where the plates are metal having a high conductivity or the relative velocity of the plates is relatively low, the film will be isothermal and $n_\gamma \cong 1$. If the relative velocities are very high the process will approach an adiabatic condition and n_γ equals the ratio of the specific heats ($n_\gamma = 1.4$ for an adiabatic process at ambient conditions).

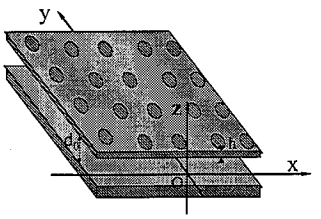

FIG. 1. A periodic perforated planar microstructure.

It is helpful to recast the equations using dimensionless variables. As the domain is the narrow air gap between the two plates (Fig. 1), we will use different scales in the x, y directions (parallel to the plane of the microstructure) and the z direction. Thus, d_0, the distance between the plates at equilibrium, will be used as a scale for the z-axis and L_0, a characteristic length connected to the planar domain for the other directions. We suppose that $\epsilon = d_0/L_0$ is a small parameter. To the lower order in ϵ and for harmonic oscillations (of frequency $\omega/2\pi$) the system describing the motion of the gas can be written as in Ref. 7

$$\frac{\partial^2 v_x}{\partial z^2} + iK^2 v_x = \frac{\partial p}{\partial x}, \tag{1}$$

$$\frac{\partial^2 v_y}{\partial z^2} + iK^2 v_y = \frac{\partial p}{\partial y}, \tag{2}$$

$$\frac{\partial p}{\partial z} = 0, \tag{3}$$

$$\nabla \cdot \mathbf{v} - i\frac{\sigma}{12 n_\gamma} p = 0, \tag{4}$$

where

$$\sigma = 12\frac{\omega \mu L_0^2}{P^a d_0^2} K = d_0 \sqrt{\frac{\rho\omega}{\mu}},$$

ρ is the equilibrium density of the gas, μ the viscosity, and P^a is the ambient pressure (atm). If V_0 is a characteristic velocity of the microstructure plane, the characteristic pressure is $P_0 = \mu V_0 L_0 / d_0^2$. Hence, the total physical pressure is

$$P^{\text{phys}} = P^a + P_0 p(x,y) e^{-i\omega t}.$$

The squeeze number σ measures the degree of compression of the fluid in the gap. If σ is close to 0 (low frequency) the air film obeys nearly incompressible viscous flow; at very high frequencies the fluid is essentially trapped in the gap and behaves like a spring.

B. Boundary conditions for gas velocity and pressure

If the gap thickness is comparable to the mean free path of the gas molecules or the pressure is lower than the ambient pressure, the tangential velocity of the fluid at the boundary is no longer strictly zero, which is called the slip-flow effect (gas rarefaction). The slip velocity on the boundary gives rise to a decrease of the viscous forces in the squeezed air film.

For including the gas rarefaction in this analysis we consider the slip velocity conditions at solid boundaries

$$v_x\left(x,y,\pm\frac{1}{2}\right) = \mp K_{\mathrm{ch}}\frac{\partial v_x}{\partial z}\left(x,y,\pm\frac{1}{2}\right),$$
$$v_y\left(x,y,\pm\frac{1}{2}\right) = \mp K_{\mathrm{ch}}\frac{\partial v_y}{\partial z}\left(x,y,\pm\frac{1}{2}\right), \tag{5}$$

Here K_{ch} is the Knudsen number introduced by Veijola in Ref. 8 as a measure of the rarefaction

$$K_{\mathrm{ch}} = \sigma_P\frac{\lambda}{d_0},$$

λ is the mean free path of the gas molecules ($\lambda = 0.068 \times 10^6/P^a$ at ambient temperature and pressure P^a). The slip coefficient σ_P, for the diffuse specular scattering model,[9] can be written as

$$\sigma_P = \frac{2-\alpha}{\alpha}[1.016 - 0.1211(1-\alpha)],$$

where α is the momentum accommodation coefficient. For diffuse scattering, $\alpha=1$ and $\alpha_P=1.016$. Also, in the direction normal to the plates the impenetrability condition yields

$$v_z\left(x,y,-\frac{1}{2}\right) = 0, \quad v_z\left(x,y,\frac{1}{2}\right) = w. \tag{6}$$

By w we denote the dimensionless Oz component of the velocity of the mobile surface, assumed a known quantity ($v_z^{\mathrm{phys}} = \epsilon V_0 w$). The classical nonslip condition can still be obtained for $K_{\mathrm{ch}}=0$. Therefore, the present analysis proves true in the continuum flow regime and in the slip flow domain as well.

In the case where the viscous loss through holes is not neglected, the pressure at the rim of the holes is assumed to be equal to a constant unknown value p_1. This gives the condition

$$p = p_1 \text{ on the rim } \partial D_D. \tag{7}$$

The pressure gradient is zero in a direction that is normal to any line of symmetry of the planar microstructure. On all symmetry lines, (denoted by δD_N) we can then write a new boundary condition as

$$\frac{\partial p}{\partial n} = 0 \text{ on } \partial D_N. \tag{8}$$

We suppose that the holes (of circular form of r_1-radius) are located at the vertices of a regular system of equilateral triangles of side length l_3(in the case of a staggered system of holes) or in the vertices of a regular system of squares, of side length l_4 for the case of aligned holes (Fig. 2). We take advantage of the repetitive pattern of the perforated plate and define a "*cell*" as the space occupied by a hole and its surrounding web space (the plane region where the hole is collecting the flow). The *basic domain D* is defined as the plane region obtained from a cell excluding the hole. The external boundary of the basic domain is a regular hexagon or a square and the inner boundary is the rim of the hole.

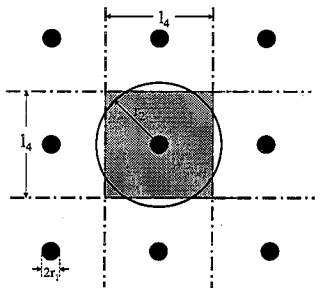

FIG. 2. The cell, the influence domain of a hole, and its circular approximation.

C. Reynolds' equation including inertia and rarefied gas effect

Since the pressure $p(x,y)$ does not depend upon z [Eq. (3)] the differential Eqs. (1)–(4) can be integrated giving the solution

$$v_x(x,y,z) = \frac{i}{K^2}\frac{\partial p}{\partial x}\left(\frac{\cos(\sqrt{i}Kz)/\cos(\sqrt{i}K/2)}{1-\sqrt{i}K_{\mathrm{ch}}K\tan(\sqrt{i}K/2)} - 1\right), \tag{9}$$

$$v_y(x,y,z) = \frac{i}{K^2}\frac{\partial p}{\partial y}\left(\frac{\cos(\sqrt{i}Kz)/\cos(\sqrt{i}K/2)}{1-\sqrt{i}K_{\mathrm{ch}}K\tan(\sqrt{i}K/2)} - 1\right), \tag{10}$$

$$v_z(x,y,z) = i\frac{\sigma}{12n_\gamma}p\left(z+\frac{1}{2}\right) + \frac{i}{K^2}\left(\frac{\partial^2 p}{\partial x^2}+\frac{\partial^2 p}{\partial y^2}\right)\times\left\{z+\frac{1}{2} - \frac{\sin(\sqrt{i}Kz)/\cos(\sqrt{i}K/2)+\tan(\sqrt{i}K/2)}{(\sqrt{i}K/2)[1-\sqrt{i}K_{\mathrm{ch}}K\tan(\sqrt{i}K/2)]}\right\}. \tag{11}$$

Here $\sqrt{i} = (1+i)/\sqrt{2}$. The second condition (6) yields the equation for the pressure

$$\frac{\partial^2 p}{\partial x^2} + \frac{\partial^2 p}{\partial y^2} + \alpha^2 p = 12Mw. \tag{12}$$

Here we have used the notations

$$\alpha^2 = iM\sigma/n_\gamma,$$
$$M = \frac{i}{12}K^2\left(\frac{\tan(\sqrt{i}K/2)}{\sqrt{i}K/2[1-\sqrt{i}K_{\mathrm{ch}}K\tan(\sqrt{i}K/2)]} - 1\right)^{-1}. \tag{13}$$

Equation (12) is the Reynolds' equation for solving the squeezing film problem in the case of a compressible gas accounting also for the influence of inertia and gas slip on the plates.

Simple numerical calculations show that $M=1$ is a good approximation for frequencies less than 100 kHz, while the expression $M = 1 - iK^2/10$ can be used for frequencies less than 10 MHz.

III. ANNULAR APPROXIMATION OF BASIC REGION

A. Determination of squeeze-film damping and hole indirect resistance

We consider an approximation of the outer boundary of the basic domain by an equivalent circle having the same

area (Fig. 2). In this case the domain D is an annulus of $r_1 < r_2$ radii. The radius of the outer circle r_2 is connected with the distance l between the holes by

$$r_2 = 0.525 l_3 \text{ or } r_2 = l_4/\sqrt{\pi},$$

due to the equality of areas. This approximation works well only in the case of small inner radius r_1 as compared with the linear dimension of the cell.[7] We take as a reference length $L_0 = r_2$ and denote $r_0 = r_1/r_2$. In polar coordinates Eq. (12) then becomes

$$\frac{1}{r}\frac{\partial}{\partial r}\left(r\frac{\partial p}{\partial r}\right) + \alpha^2 p = 12Mw, \quad for \quad r_0 < r < 1. \tag{14}$$

The boundary conditions for the function $p(r)$ are

$$p(r_0) = p_1, \quad \frac{\partial p}{\partial r}(1) = 0. \tag{15}$$

The solution of Eq. (14) satisfying the conditions (15) can be written as

$$p(r) = \frac{12 n_\gamma w}{i\sigma}\left[1 - \left(1 - i\frac{\sigma}{12 n_\gamma} p_1^0\right) \times \frac{Y_1(\alpha)J_0(\alpha r) - J_1(\alpha)Y_0(\alpha r)}{Y_1(\alpha)J_0(\alpha r_0) - J_1(\alpha)Y_0(\alpha r_0)}\right], \tag{16}$$

where $p_1 = p_1^0 w$ and J_0, J_1, Y_0, Y_1 are the Bessel functions of the first and second kind.

We have also

$$\int\int_{D_1'} p(r)\,dx\,dy = -12\pi M C(\alpha, r_0) w, \tag{17}$$

where

$$C(\alpha, r_0) = C^{(0)}(\alpha, r_0) - \frac{p_1^0}{12M} C^{(1)}(\alpha, r_0),$$

$$C^{(0)}(\alpha, r_0) = \frac{1}{\alpha^2}\left(\frac{2r_0}{\alpha}\frac{J_1(\alpha)Y_1(\alpha r_0) - Y_1(\alpha)J_1(\alpha r_0)}{Y_1(\alpha)J_0(\alpha r_0) - J_1(\alpha)Y_0(\alpha r_0)} - 1 + r_0^2\right),$$

$$C^{(1)}(\alpha, r_0) = \frac{2r_0}{\alpha}\frac{J_1(\alpha)Y_1(\alpha r_0) - Y_1(\alpha)J_1(\alpha r_0)}{Y_1(\alpha)J_0(\alpha r_0) - J_1(\alpha)Y_0(\alpha r_0)}. \tag{18}$$

The total pressure on the domain D_1' in Eq. (17) contains two terms: the first term corresponding to $C^{(0)}(\alpha, r_0)$ is the squeezed film damping and the second one, involving the function $C^{(1)}(\alpha, r_0)$, is the indirect resistance of the holes.

In the case $|\alpha^2| \ll 1$, which corresponds to a weak compressible fluid and low to moderate frequencies, where the power series expansion can be used

$$\frac{2r_0}{\alpha}\frac{J_1(\alpha)Y_1(\alpha r_0) - Y_1(\alpha)J_1(\alpha r_0)}{Y_1(\alpha)J_0(\alpha r_0) - J_1(\alpha)Y_0(\alpha r_0)} = 1 - r_0^2 + c_0\alpha^2 + c_1\alpha^4 + O(\alpha^6),$$

where

$$c_0(r_0) = \frac{r_0^2}{2} - \frac{3}{8} - \frac{r_0^4}{8} - \frac{1}{2}\ln r_0,$$

$$c_1(r_0) = \frac{11}{64} - \frac{5r_0^2}{16} + \frac{11r_0^4}{64} - \frac{r_0^6}{32} + \frac{3}{8}\ln r_0 + \frac{1}{4}(\ln r_0)^2 - \frac{r_0^2}{4}\ln r_0.$$

Therefore,

$$C^{(0)}(\alpha, r_0) = c_0(r_0) + c_1(r_0)\alpha^2 + O(\alpha^4),$$
$$C^{(1)}(\alpha, r_0) = 1 - r_0^2 + c_0(r_0)\alpha^2 + c_1(r_0)\alpha^4 + O(\alpha^6). \tag{19}$$

The total force on the domain D due to the squeeze-film damping and indirect hole resistance can be written as

$$F^s = 12\frac{\pi\mu r_2^4}{d_0^3} M C(\alpha, r_0) w^{\text{phys}}. \tag{20}$$

If the first boundary condition (15) is changed to $p(r_0) = 0$, Eq. (20) gives only the squeeze-film damping.

For an incompressible fluid ($\alpha = 0$) and for small or moderate frequencies, the resulting expression for the squeeze-film damping reduces to

$$F^{\text{inc}} = \frac{12\pi\mu r_2^4}{d_0^3}\left(\frac{1}{2}r_0^2 - \frac{1}{8}r_0^4 - \frac{1}{2}\ln r_0 - \frac{3}{8}\right) w^{\text{phys}}, \tag{21}$$

which coincides with Škvor's formula.[10,11]

B. Application to analysis of an ultrasonic transducer

The ultrasonic transducer developed in Ref. 6 consists of an array of diaphragms connected in parallel. The capacitive diaphragm has a hexagonal shape (of 45 μm side length) and contains 5 μm square holes spaced on a square 30 μm grid. The gap between upper and lower polysilicon electrodes is 2.0 μm and the upper polysilicon electrode thickness is 2.0 μm. The measured resonant frequency is 3.47 MHz.

In order to estimate parameters for a single degree of freedom (SDOF) dynamic model, the hexagonal diaphragm was replaced with a simply supported circular diaphragm having the same resonant frequency. The equivalent SDOF mass is $m^* = 4.87 \times 10^{-12}$ kg, the SDOF spring constant $k^* = 2.33 \times 10^3$ N/m, and the equivalent area is $S^* = 1.06 \times 10^{-9}$ m^2 for a single diaphragm.

The damping is characterized by two terms. The first term describes the contribution of the radiation of ultrasonic energy. The radiation of acoustic energy across the equivalent SDOF area S^* yields a quality factor given by

$$Q_{\text{radiation}} = \frac{\sqrt{m^* k^*}}{Z_{\text{air}} S^*} = 233,$$

where the acoustic impedance of air $Z_{\text{air}} = 430$ N$-$s/m^2 and where m^*, K^*, and S^* from the SDOF model have been used.

The other contribution to the damping comes from the squeeze-film damping. In Ref. 6 the squeeze-film damping was calculated by using the lubrication approximation for an incompressible fluid. In the model, each grid square was re-

placed with a circular piston traveling within a cylinder, having outer radius $r_1=16.9$ μm and a central circular vent hole of inner radius $r_2=2.82$ μm, preserving the area in one grid square. The analysis, similar to Škvor's approach, yields the total force acting against the face of the piston as $F=3.65\times10^{-6}\ w^{\text{phys}}$, describing an equivalent viscous damper with dashpot constant $c=3.65\times10^{-6}$ N−s/m.

In the model, the authors consider the five etch holes nearest the center to represent the location of discrete dashpots that are transformed into one equivalent SDOF dashpot by summing the product of each dashpot constant by the square of the mode shape at each etch hole location. In this geometry, the equivalent SDOF dashpot constant is $c^*=4.15\times10^{-6}$ N−s/m. The one vent hole at the center, where the mode shape amplitude is 1.0, is the dominant contributor to the equivalent dashpot constant, because the diaphragm velocity at the four next nearest dashpots, each 30 μm away from the center, is very low. The quality Q factor associated with the squeeze film damping effect for the SDOF is then obtained as

$$Q_{\text{squeeze-film}}=\omega_0\frac{m^*}{c^*}=29.1, \tag{22}$$

leading to a predicted combined Q value calculated as

$$Q=\left[\frac{1}{Q_{\text{radiation}}}+\frac{1}{Q_{\text{squeeze-film}}}\right]^{-1}=25.9. \tag{23}$$

The measured value of the quality factor is $Q_{\text{mes}}=49.6$ at atmospheric pressure.

By taking into consideration the compressibility of the air, the inertia effect and the rare gas effect formula (20) (corresponding to the case $p_1=0$) yields the total force acting against the face of the piston as $F=2.6\times10^{-6}\ w^{\text{phys}}$. In the given geometry the equivalent SDOF dashpot constant is $c^*=2.96\times10^{-6}$ N−s/m. Correspondingly, $Q_{\text{squeeze-film}}$ determined by formula (22) has the value 35.9, which introduced in formula (23) gives the predicted combined quality factor $Q=42.44$.

Thus the consideration of compressibility, inertia, and rare gas effects reduced the difference between the predicted and measured quality factor of the damping of the diaphragm of the transducer from 48% to 14%.

IV. TOTAL VISCOUS DAMPING AND SPRING FORCE

A. Direct hole resistance

In this section, we extend the results presented above by determining the direct resistance of the flow through holes. As in the above formulation, the effects of compressibility, inertia, and gas rarefaction will be accounted for. The last effect is determined by the breakdown of the continuum behavior of the gas determined by the narrowness of the holes or by the drop of the pressure under the ambient pressure. In order to determine the "*resistance of the holes*" we assume a pressure p_1 along the upper edge of a perforation and model a plate hole as a pipe of diameter $2r_1$ and of length h equal to the plate thickness. In this case the only nonvanishing component of velocity in the hole is v_z (fully developed *Poiseuille flow*).[12] We can then write the equation

$$\Delta v_z+\frac{i\omega}{\nu}v_z=\frac{1}{\mu}\frac{\partial p}{\partial z},$$

$\nu=\mu/\rho$ being the dynamic viscosity. In polar coordinates this becomes

$$\frac{1}{r}\frac{\partial}{\partial r}\left(r\frac{\partial v_z}{\partial r}\right)+\frac{i\omega}{\nu}v_z=\frac{p_1}{\mu h}, \tag{24}$$

an equation similar to Eq. (14). Its solution, finite in the domain $r<r_1$, also has to satisfy the following boundary condition on the pipe wall $r=r_1$:

$$v_z(r_1)=-K_{\text{tb}}r_1\frac{\partial v_z(r_1)}{\partial r}, \tag{25}$$

where

$$K_{\text{tb}}=\sigma_P\frac{\lambda}{r_1}$$

is the other Knudsen number introduced in Ref. 13 as a measure of the rarefaction in a pipe.

The solution of Eq. (24) satisfying the condition (25) is

$$v_z=\frac{p_1}{i\omega\rho h}\left[1-\frac{J_0(\beta r)}{J_0(\beta r_1)-K_{\text{tb}}\beta r_1 J_1(\beta r_1)}\right], \tag{26}$$

where $\beta^2=i\omega/\nu$. The total volume rate of flow results by integration in the form

$$Q^h=-\frac{\pi p_1 r_1^4}{8\mu h}H(\beta r_1), \tag{27}$$

where

$$H(\beta r_1)=\frac{8}{(\beta r_1)^2}(G(\beta r_1)-1),$$

$$G(\beta r_1)=\frac{2}{\beta r_1}\frac{J_1(\beta r_1)}{J_0(\beta r_1)-K_{tb}\beta r_1 J_1(\beta r_1)}.$$

The wall shear stress can be shown to be

$$\tau=-\mu\frac{dv_z}{dr}(r_1).$$

By using Eq. (26) for the velocity this becomes

$$\tau=-\frac{p_1 r_1}{2h}G(\beta r_1). \tag{28}$$

The direct resistance of the holes F_d^h is obtained by integrating the wall shear stress (28) along the boundary of the pipe. There results

$$F_d^h=-\pi r_1^2 p_1 G(\beta r_1). \tag{29}$$

Remark 1 *In the case where the thickness of the plate h and the radius r_1 are of comparable dimensions a correction has to be made for the effect of the end of the hole. Sharipov and Seleznev, in Ref. 9, have shown that this effect can be included in Eq. (29) by replacing the length h of the hole with*

$$h_{\text{eff}}=h+3\pi r_1/8.$$

Finally, the total viscous damping on a cell is obtained by adding the two viscous forces given by formulas (20) and (29)

$$F^T = F^s = \left[12\frac{\pi\mu r_2^4}{d_0^3} MC(\alpha, r_0) - \pi r_1^2 p_1^0 G(\beta r_1) \right] w^{\text{phys}}. \tag{30}$$

B. Determination of rim pressure p_1

The compressibility of the gas makes the determination of the rim pressure p_1 more difficult. Thus, the linearized continuity Eq. (4) can be written in dimensional variables as

$$\nabla \cdot \mathbf{v} = \frac{i\omega}{n_\gamma P^a} p. \tag{31}$$

The integration of Eq. (31) over the 3D space D_3 between the microstructure plates corresponding to a cell (in its cylindrical approximation) yields

$$\int\int_{\partial D_3} \mathbf{v} \cdot \mathbf{n} dS = \frac{i\omega d_0}{n_\gamma P^a} \int\int_{D \cup D_1} p dS.$$

Here D is the basic 2D domain (considered on the lower plate) and the plane domain D_1 corresponds to the holes' entrance. Hence,

$$\pi r_2^2 w^{\text{phys}} - \int\int_{D_1} v_z(x,y,0) dx dy = \frac{i\omega d_0}{n_\gamma P^a} \left\{ \int\int_D p dS + \pi r_1^2 p_1 \right\}. \tag{32}$$

Now, defining $p_1 = p_1^0 w^{\text{phys}}$, and noting that the integral in left-hand side of Eq. (32) is given by formula (27) and the integral in the right-hand side by formula (20), we obtain

$$r_2^2 + \frac{r_1^4}{8\mu h} H(\beta r_1) p_1^0 = \frac{i\omega d_0}{n_\gamma P^a} \left\{ -\frac{12\mu r_2^4}{d_0^3} MC^{(0)} + \frac{\mu r_2^4}{d_0^3} C^{(1)} p_1^0 + r_1^2 p_1^0 \right\}.$$

Finally, the rim pressure is given by

$$p_1 = -\frac{r_2^2 + 12 i \mu r_2^4 \Omega MC^{(0)}}{r_1^4 H(\beta r_1)/(8\mu h) - i\Omega[\mu r_2^4 C^{(1)} + d_0^3 r_1^2]} w^{\text{phys}},$$

where

$$\Omega = \frac{\omega}{n_\gamma P^a d_0^2}.$$

C. Example

As an example we consider a capacitive diaphragm (having the velocity 1 m/s) of thickness 2.0 μm having a regular pattern of holes of radius $r_2 = 2.82$ μm and having the equivalent radius of the external circle $r_1 = 16.9$ μm. The gap equals 2 μm. The calculation of the total force on a cell was performed in the range of frequencies from 100 Hz to 1 MHz. In order to clarify which of the effects studied in this paper are of most importance to designers, some of the results are shown in Fig. 3, where the continuous line represents the damping force and the dotted line the spring force in the case where all the effects (inertia, compressibility, and slip on the boundary due to rarefaction) are included. The case of the no-slip boundary condition (without the rarefaction correction) is also presented in Fig. 3 as (–·–) for the damping force and (–···–) for the spring force. In this case the differences are very small. In the case of smaller gaps this correction could be more important. The damping force dominates at low frequencies. The cutoff frequency is slightly lower than 3 kHz. For higher frequencies the spring force dominates. The graph is very similar to Fig. 2 in Veijola's paper,[8] where the author has considered a modified Reynolds equation including the effect of inertial forces and rare gas in the relative flow-rate coefficient and has applied this equation to a squeezed-film damper model for a rectangular geometry. This shows that a cell of a regular perforated microstructure has the same mechanical behavior as a function of frequency as an open rectangular (unperforated) plate. To investigate the influence of compressibility we plotted in Fig. 4 the same elements as in Fig. 3 in the case of incompressible fluid. The damping force is in this case independent of frequency while the spring force is increasing linearly with frequency. For all the frequencies between 100 Hz and 1 MHz the spring force is much smaller than the damping force. There is a small increase in damping force due to the rarefaction effect but, practically, the spring force is not affected by the slip condition on solid boundaries. The effect of inertia can be also seen in Figs. 3 and 4 as a dependence on frequency. In the case of incompressible fluids and also for small frequencies in the compressible case, the damping force is independent of inertia.

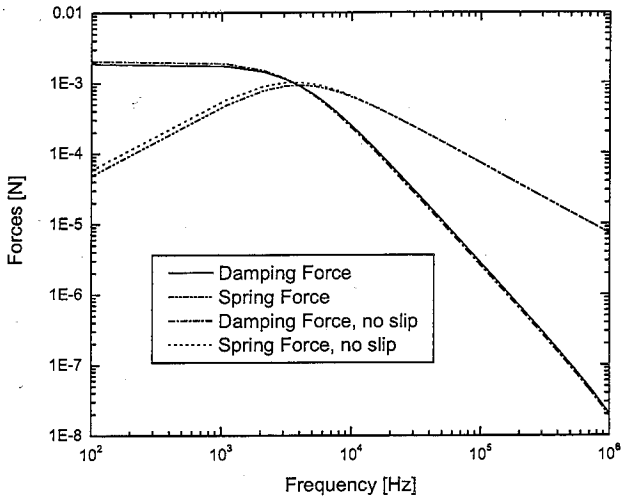

FIG. 3. The variation of the total damping and spring forces for a cell with frequency in the case of slip and no-slip boundary conditions.

V. CONCLUSIONS

This paper provides analytical formulas for the squeeze film damping, the direct and indirect resistances due to holes,

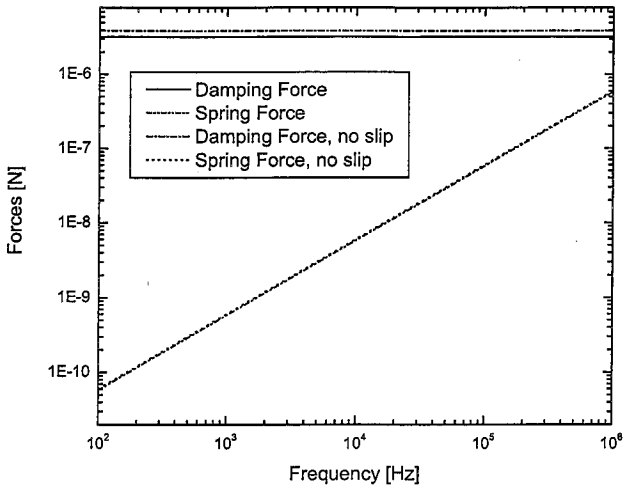

FIG. 4. The variation of the total damping force and spring force for a cell with frequency for incompressible fluids in the case of slip and no-slip boundary conditions.

and the corresponding spring forces for a periodic perforated microstructure including the effects of compressibility, inertia, and rarefied gas.

The total damping and spring forces are obtained by using the continuity equation.

Consideration of compressibility, inertia, and rarefied gas effects have reduced the error in predicting the quality factor of the damping of the diaphragm of the ultrasonic transducer analyzed in Sec. III B from 48% to 14% as compared with the measured value.

The total damping and spring forces for a cell are very similar to those corresponding to a rectangular open microstructure without holes. The separate analysis of each special correction shows that the largest correction is given by accounting for compressibility. The effect of inertia can be considered as important for the spring force and for the damping for sufficiently high frequencies. The rarefaction correction for the gaps larger than 2 μm is very small.

ACKNOWLEDGMENT

This work has been supported through NIH Grant No. R01 DC05762-1A1 to R.N.M.

[1]J. J. Blech, "On isothermal squeeze films," J. Lubr. Technol. **105**, 615–620 (1983).
[2]T. B. Gabrielson, "Mechanical-thermal noise in micromachined acoustic and vibration sensors," IEEE Trans. Electron Devices **40**, 903–909 (1993).
[3]M. Gad-el-Hak, editor, *MEMS Applications* (CRC Press, Taylor & Francis Group, Boca Raton, FL, 2006).
[4]M. Andrews, I. Harris, and G. Turner, "Compařison of squeeze-film theory with measurements on a microstructure," Sens. Actuators, A **36**, 79–87 (1993).
[5]D. Homentcovschi and R. N. Miles, "Viscous microstructural dampers with aligned holes: Design procedure including the edge correction," J. Acoust. Soc. Am. **122**, 1556–1567 (2007).
[6]I. J. Oppenheim, A. Jain, and D. W. Greve, "Electrical characterization of coupled and uncoupled MEMS ultrasonic transducers," IEEE Trans. Ultrason. Ferroelectr. Freq. Control **50**, 297–304 (2003).
[7]D. Homentcovschi and R. N. Miles, "Viscous damping of perforated planar micromechanical structures," Sens. Actuators, A **119**, 544–552 (2005).
[8]T. Veijola, "Compact models for squeezed-film dampers with inertial and rarefied gas effects," J. Micromech. Microeng. **14**, 1109–1118 (2004).
[9]M. H. Shapirov and V. Seleznev, "Data on internal rarefied gas flows," J. Phys. Chem. Ref. Data **27**, 657–706 (1997).
[10]Z. Škvor, "On acoustical resistance due to viscous losses in the air gap of electrostatic transducers," Acustica **19**, 295–297 (1967–1968).
[11]D. Homentcovschi and R. N. Miles, "Modelling of viscous damping of perforated planar micro-mechanical structures. Applications in acoustics," J. Acoust. Soc. Am. **116**, 2939–2947 (2004).
[12]F. M. White, *Viscous Fluid Flow* (McGraw–Hill, New York, 1992).
[13]T. Veijola, "Analytic damping model for an MEM perforation cell," Microfluid. Nanofluid. **2**, 249–260 (2006).